THE JOURNAL OF BIOLOGICAL CHEMISTRY VOL. 283, NO. 9, pp. 5510–5517, February 29, 2008

Characterization of a Protein Phosphatase 2A Holoenzyme That Dephosphorylates the Clathrin Adaptors AP-1 and AP-2*[S]

Received for publication, August 27, 2007, and in revised form, December 12, 2007 Published, JBC Papers in Press, December 24, 2007, DOI 10.1074/jbc.M707166200

Doris Ricotta[‡1], **Jens Hansen**[§1,2], **Carolin Preiss**[§], **Dominic Teichert**[¶], **and Stefan Höning**[§3]

From the [‡]*Department of Biomedical Science and Biotechnology, University of Brescia, 25100 Brescia, Italy,* [§]*Institute for Biochemistry II, University of Göttingen, 37073 Göttingen, Germany, and* [¶]*Institute for Biochemistry I, University of Cologne, 50931 Cologne, Germany*

The AP-2 complex is a key factor in the formation of endocytic clathrin-coated vesicles (CCVs). AP-2 sorts and packages cargo membrane proteins into CCVs, binds the coat protein clathrin, and recruits numerous other factors to the site of vesicle formation. Structural information on the AP-2 complex and biochemical work have allowed understanding its function on the molecular level, and recent studies showed that cycles of phosphorylation are key steps in the regulation of AP-2 function. The complex is phosphorylated on both large subunits (α- and β2-adaptins) as well as at a single threonine residue (Thr-156) of the medium subunit μ2. Phosphorylation of μ2 is necessary for efficient cargo recruitment, whereas the functional context of the large subunit phosphorylation is unknown. Here, we show that the subunit phosphorylation of AP-2 exhibits striking differences, with calculated half-lives of <1 min for μ2, ~25 min for β2, and ~70 min for α. We were also able to purify a phosphatase that dephosphorylates the μ2 subunit. The enzyme is a member of the protein phosphatase 2A family and composed of a catalytic Cβ subunit, a scaffolding Aβ subunit, and a regulatory Bα subunit. RNA interference knock down of the latter subunit in HeLa cells resulted in increased levels of phosphorylated adaptors and altered endocytosis, showing that a specific PP2A holoenzyme is an important regulatory enzyme in CCV-mediated transport.

Internalization from the plasma membrane occurs by different pathways, including uptake via clathrin-coated vesicles (CCVs).[4] Although it is obvious that clathrin coat assembly and disassembly need to be tightly regulated both spatially and temporally, little was known until now about the respective mechanisms that control the function of the many factors that are identified. However, increasing evidence suggests that cycles of phosphorylation/dephosphorylation are key events in the regulation of endocytic proteins (1). Indeed, the major endocytic CCV constituents, clathrin and AP-2, are functionally regulated by phosphorylation, as well as other factors including dynamin 1, amphiphysins, synaptojanin, AP180, epsin, and eps15, which are collectively grouped as dephosphins, that become active in their dephosphorylated state (2).

Because AP-2 is a key factor in the formation of CCVs and known for a long time to be phosphorylated, it is an ideal model protein to analyze the functional consequences and regulatory mechanisms of cycles of phosphorylation (3). The complex is phosphorylated on the medium subunit μ2 at a single threonine residue (Thr-156), which is mediated *in vitro* by the two kinases AAK1 and GAK (4–8). Both kinases phosphorylate not only μ2 but also the μ1 subunit of the AP-1 complex *in vitro*, and it is yet unclear whether the two kinases act redundantly or distinctively (9, 10). Besides this uncertainty, the current data show that phosphorylation of the adaptor μ subunits is a trigger for high affinity binding to YXXΦ sorting signals of cargo membrane proteins (5, 11).

Although there is no evidence for phosphorylation of the AP-2 σ2 subunit, both large subunits (α- and β2-adaptins) are phosphorylated, but it is not well established which residues are modified. Using a phosphotyrosine-specific antibody, Sorkin and coworkers identified an amino-terminal tyrosine (Tyr-6) as a major target site for β2 phosphorylation (12), whereas more recently others have identified Tyr-737 located in the ear domain as an agonist-dependent Src kinase target (13). Not only tyrosine residues have been identified as phosphorylation target sites but also serine/threonine kinases such as the recently identified CVAK104 (14) may impact on the phosphorylation status of β2-adaptin. Likewise, α-adaptin is also phosphorylated, but no data are available on the target sites and the involved kinase(s).

To get further insight into the role of AP-2 phosphorylation, we used pulse-chase experiments to determine the phosphorylation turnover of the different AP-2 subunits. To our surprise, the phosphorylation half-lives exhibited great differences, ranging from <1 min in the case of μ2 to 25 min for β2 and ~70 min for the α subunit. In addition, we purified a μ2-dephosphorylating enzyme activity from pig brain to homogeneity. The

* This work was supported by grants from the Deutsche Forschungsgemeinschaft (SFB523, TPA5; SFB635, TPA3) (to S. H.). The costs of publication of this article were defrayed in part by the payment of page charges. This article must therefore be hereby marked "*advertisement*" in accordance with 18 U.S.C. Section 1734 solely to indicate this fact.

[S] The on-line version of this article (available at http://www.jbc.org) contains supplemental Fig. S1 and a supplemental model.

[1] Both authors contributed equally to this work.

[2] Present address: Inst. for Clinical Chemistry and Laboratory Medicine, University of Regensburg, Germany.

[3] To whom correspondence should be addressed: Inst. of Biochemistry I, University of Cologne, Joseph-Stelzmann-Str. 52, 50931 Cologne, Germany. Tel.: 49-221-4783656; Fax: 49-221-4786979; E-mail: shoening@uni-koeln.de.

[4] The abbreviations used are: CCV, clathrin-coated vesicle; PP2A, protein phosphatase 2A; RNAi, RNA interference; PBS, phosphate-buffered saline; Tf, transferrin.

enzyme was identified as a protein phosphatase 2A (PP2A) and composed of all three subunits that constitute a functional holoenzyme: a catalytic Cβ subunit, a scaffolding Aβ subunit, and a regulatory Bα subunit. Because the latter subunit is assumed to determine intracellular location and substrate specificity, we knocked down the PP2A Bα subunit in HeLa cells by RNAi. In the affected cells, we detected increased levels of μ2 phosphorylation and altered endocytosis of transferrin, showing that a particular PP2A is an important regulatory enzyme in CCV-mediated transport.

EXPERIMENTAL PROCEDURES

Reagents and Antibodies—Monoclonal anti-α-adaptin was from Alexis; antibodies against the PP2A subunits were from Santa Cruz Biotechnology (rabbit anti-PP2A Cα/β; rabbit anti-PP2A Aα/β; rabbit anti-PP1; rabbit anti-PP2B) and Millipore GmbH (Schwalbach, Germany) (monoclonal anti-Bα). Phosphorylated μ2 was detected with sheep antibodies (kindly provided by Elizabeth Smythe, University of Sheffield, UK) or with serum from a rabbit that was immunized with a synthetic peptide comprising phosphorylated Thr-156. Monoclonal antibodies against clathrin and γ-adaptin were from BD Transduction Laboratories; anti-tubulin was from Molecular Probes. Horseradish peroxidase-conjugated secondary antibodies used for Western blotting and fluorochrome-labeled antibodies were from Dianova (Hamburg, Germany). Protein phosphatase 1, 2A, and 2B proteins were obtained from Calbiochem. The serine/threonine kinase inhibitor staurosporine was from Sigma; the phosphatase inhibitors ocadaic acid and calyculin-A were from Alexis; microcystin-agarose was obtained from Upstate.

Cell Culture—HeLa and MDBK cells were grown at 37 °C under standard cell culture conditions at 5% CO_2 in Dulbecco's modified Eagle's medium supplemented with 10% fetal calf serum. Cells derived from transfection with the PP2A B-α RNAi vector were maintained in the presence of 200 μg/ml G-418.

Purification of CCVs and Immunoisolation of AP-2—The CCV preparation and the AP-2 purification from them, as well as the ^{32}P labeling of AP-2 and its immunoisolation, were exactly as described (5, 15).

In Vitro Dephosphorylation of AP-2—^{32}P-labeled AP-2 (10–15.000 cpm) was incubated in 50 mM Tris-HCl, pH 7.2, 100 mM NaCl, 1 mM dithiothreitol for 30 min at 37 °C without any further additions (negative control) or with pig brain or HeLa cytosol (5–100 μg) or commercial protein phosphatase (0.05 units/sample) in a final volume of 100 μl. Subsequently, the samples were centrifuged, the supernatants were removed, and the immunoadsorbed AP-2 was washed three times with dephosphorylation buffer followed by SDS-PAGE and subsequent detection with autoradiography and Western blotting.

Purification of an AP-2-Dephosphorylating Enzyme from Pig Brain—Pig brain cytosol obtained from the CCV purification was precipitated with $(NH_4)_2SO_4$ (35% final concentration), followed by centrifugation at 10,000 rpm for 20 min in a JA10 rotor (Beckman Coulter). The derived supernatant was dialyzed against buffer A (50 mM Tris, pH 7.4, 2 mM $MgCl_2$, 0.1 mM EGTA, 1.5 M $(NH_4)_2SO_4$), followed by centrifugation as described above. The fractionated cytosol was then applied to hydrophobic interaction chromatography on a phenyl-Sepharose column (1 × 30 cm) equilibrated in buffer A and connected to a Perseptive Vision chromatography work station at a flow rate of 4 ml/min. After sample application, the column was extensively washed for 1 h with buffer A followed by gradient elution using buffer A without ammonium sulfate. The μ2-phosphorylating activity was collected in the third of three peaks eluting at the end of the gradient. The fractions were pooled and dialyzed against buffer B (50 mM Tris, pH 7.4, 2 mM $MgCl_2$, 0.1 mM EGTA, 5% glycerol), followed by strong anion exchange chromatography using a 4.6 × 100-mm Source Q column at a flow rate of 5 ml/min. After washing of the column with 10 column volumes, proteins were eluted with a NaCl gradient (0–0.5 M within 15 column volumes). The μ2-dephosphorylating activity eluted in two consecutive fractions at ~250 mM salt. The fractions were pooled and dialyzed against buffer B, followed by chromatography on a 4.6 × 100-mm DEAE-Sepharose column equilibrated in buffer B at a flow rate of 1 ml/min. The μ2-dephosphorylating activity was collected in two fractions eluting at ~600 mM salt. Fractions were pooled (2 ml) and concentrated to 200 μl by centrifugation and then applied to size exclusion chromatography using a 7.8 × 300-mm G3000 SWXL column (Toso Haas) equilibrated in buffer B at a flow rate of 0.5 ml/min. Only one major peak was detectable that contained the μ2-dephosphorylating activity and eluted at a size of ~200 kDa. The eluted protein sample was kept at 4 °C until further use.

Immunoprecipitation of Cellular Adaptors—Pulse-chase experiments were used to immunoprecipitate intracellular phospho-AP-2. In brief, confluent cells on 3-cm dishes were starved in phosphate-free medium followed by incubation with 220 μCi [^{32}P]orthophosphate in 1 ml of phosphate-free Dulbecco's modified Eagle's medium (5% serum) for 8.5 h (pulse). Afterward, the labeling medium was removed and the cells were washed and subsequently incubated for the indicated chase periods in Dulbecco's modified Eagle's medium containing 10-fold excess phosphate. Control cells (t = 0 min) were collected after the pulse. All incubations were stopped by transferring the cells on ice and immediately exchanging the medium for ice-cold homogenization buffer (25 mM Tris, 150 mM NaCl, 1 mM EDTA, pH 7.2). The cells were scraped in 1 ml of homogenization buffer, collected by centrifugation for 5 min with 500 × g, and then resuspended in 0.5 M Tris, 150 mM NaCl, 1 mM EDTA, pH 7.2, 1% Triton X-100, 10 nM calyculin, 10 nM okadaic acid, 400 nM cantharidin, 900 nM endothal, protease inhibitors and incubated for 30 min, followed by centrifugation for 30 min at 100,000 × g to remove insoluble proteins. AP-2 was immunoprecipitated from the supernatants as described (5) and resolved by conventional or 6 M urea-containing SDS-PAGE (16). The subunit-incorporated radioactivity was quantified from the dried gels using a FUJIX BAS 1000. In some experiments AP-1 was precipitated as described above, using monoclonal anti-γ adaptin antibodies.

The amount of radioactivity present in the labeling medium before/after the pulse and in the medium after the chase was determined by Cerenkov counting. By subtracting the values, the intracellular radioactivity after the chase was determined. For each experiment, the sums over time of the values of α, β2,

and μ2 phosphorylation and intracellular radioactivity were determined. To level these values from different experiments, they were multiplied with a factor so that the corresponding sums in each experiment were the same. Average values and standard deviations were then generated and expressed in percent of the control average values ($t = 0$ min). Intracellular radioactivity was interpolated with the sum of two e-functions and differentiated, and the differentiation was expressed in percent of control, too. The phosphorylation half-lives were determined as described in the supplemental information. For the data evaluation, Microsoft Excel and R program were used. Data were interpolated with the formulas after the method of least squares using the function "nls" in the R program.

Identification of Proteins by Mass Spectrometry—For peptide mass fingerprint analysis, the respective protein bands visible after Coomassie staining were excised, cut in 1-mm small pieces and subjected to in-gel digestion with trypsin (17), desalted on C18 ZipTIP, and analyzed by matrix-assisted laser desorption ionization time-of-flight mass spectrometry using dihydrobenzoic acid as matrix and two autolytic peptides of trypsin (m/z 842.51 and 2211.10) as internal standards. The mass spectrometric data were used by Mascot search algorithm for protein identification in the NCBInr protein data base.

Suppression of PP2A Bα by RNA Interference—A plasmid-based system was used to stably suppress the expression of the PP2A Bα subunit in HeLa cells. The sequence GAACCCACTTCCTGCTTAG starting at position 1667 in the 3′-untranslated region of the human Bα mRNA (NM_002717) was used as a target. In brief, two complementary oligonucleotides were synthesized containing the above target sequence followed by a spacer of nine nucleotides, the target sequence in reverse orientation, and a sequence of five thymidine bases as a terminator of transcription. Both primers were annealed and cloned into the pSHH plasmid (BioCarta) using SalI and XbaI restriction sites. The plasmid, which also confers resistance to G418, was transfected into HeLa cells using Effectene (Qiagen) as a transfection reagent. Single clones were assayed by Western blotting for suppression of the Bα subunit. Three clones in which Bα expression was reduced by more than 80% were used for further analysis. No obvious variation between the clones was noticeable. To rule out unwanted side effects of vector-based RNAi for the PP2A Bα subunit, we also used small interference RNA oligos for the same and an additional target sequence (GTCTCATAGCAGAGGAGAA).

For rescue experiments, the coding sequence of the human Bα-cDNA was cloned in-frame into the pCMV-3Tag-6 vector (Stratagene) using HindIII and XhoI restriction sites. The final insert codes for an amino-terminal triple repeat of the FLAG tag (25 amino acids), followed by an additional spacer sequence (30 amino acids) that was found to be essential for detection of the tag sequence. Expression from the vector in HeLa cells was not sensitive to the target sequence of vector-based RNAi and the respective small interference RNA oligos, because the target sequences in the 3′-untranslated region were deleted from the insert. The recombinant 3× FLAG-tagged Bα subunit was detected by using tag-specific monoclonal (GenScript) or polyclonal (Delta Biolabs) antibodies. Integration of the tagged recombinant Bα subunit into PP2A holoenzymes was verified by detection of the PP2A C and A subunits in anti-FLAG antibody immunoprecipitates and by detection of the recombinant subunit after capture of PP2A using agarose-immobilized microcystin (see supplemental Fig. S1).

Endocytosis Experiments—Cells on glass coverslips were serum-starved for 1 h in Dulbecco's modified Eagle's medium with 0.5% serum albumin, washed with PBS, and incubated for 15 min on ice in the presence of 20 μg/ml Alexa 546-conjugated human transferrin (Tf), human Dil-LDL (20 μg/ml), or rhodamine-labeled dextran (2 mg/ml). Afterward, the cells were either immediately fixed and processed for microscopy or first incubated at 37 °C for 5 min to 2 h to monitor internalization.

For the biochemical analyses of Tf uptake, we used the biotinylated protein. Parallel samples were incubated on ice with Biotin-Tf for 30 min followed by washing with PBS. Then one sample was collected for subsequent analysis of the total amount of bound Tf. A second sample was left on ice and later subjected to trypsin treatment to control the removal of surface Tf. All other samples were incubated at 37 °C for up to 10 min and then chilled on ice, washed with PBS, and incubated three times for 5 min with trypsin to remove surface Tf. After washing with PBS, 1% serum, the cells of all samples were scraped, collected by centrifugation, and homogenized in PBS, 1% Triton X-100. Subsequently, the biotin-Tf was immunoprecipitated with streptavidin-agarose and detected by Western blotting. A concentration series of biotin-Tf served as a control for the amount of cell-internalized protein. Trypsin treatment was able to remove >95% of all surface Tf. Endocytosis is expressed as the amount of cell-associated biotin-Tf relative to the total amount initially bound on ice.

Immunofluorescence—Cells were seeded on glass coverslips 1 or 2 days before use. After fixation with 3% paraformaldehyde for 20 min and blockage of remaining aldehyde groups with 50 mM NH_4Cl in PBS for 10 min, the cells were permeabilized using 0.5% saponin in PBS. Incubation with the primary antibodies was carried out for 1 h at 37 °C, followed by incubation for 15 min in 10% goat serum and incubation with the fluorochrome-conjugated secondary antibodies for 30 min at 37 °C. After washing with PBS and water, the samples were mounted in Fluoromount (DAKO) and analyzed with a confocal laser scanning microscope (Leica TCS-2 AOBS). For quantitative analysis we determined the fluorescence intensity along identical longitudes of plasma membrane profiles in an area of 200 × 200 μm in HeLa and RNAi cells.

Miscellaneous—For inhibition of μ2 dephosphorylation by PP2A, a synthetic Thr-phosphorylated peptide was used ($CQ^{148}SQITSQVT^{P}GQIGWR^{162}$) that resembles the phosphorylation site in the AP-2 μ2 subunit with an additional cysteine at the amino terminus. The equivalent non-phosphorylated peptide and two other non-related peptides were used as controls.

RESULTS AND DISCUSSION

The AP-2 Subunits Exhibit Different Phosphorylation Turnover Rates—To gain insight into the phosphorylation turnover of the different AP-2 subunits, cells were labeled with [^{32}P]phosphate for 8.5 h to mark a large pool of proteins. After labeling, AP-2 was either immediately immunoprecipitated

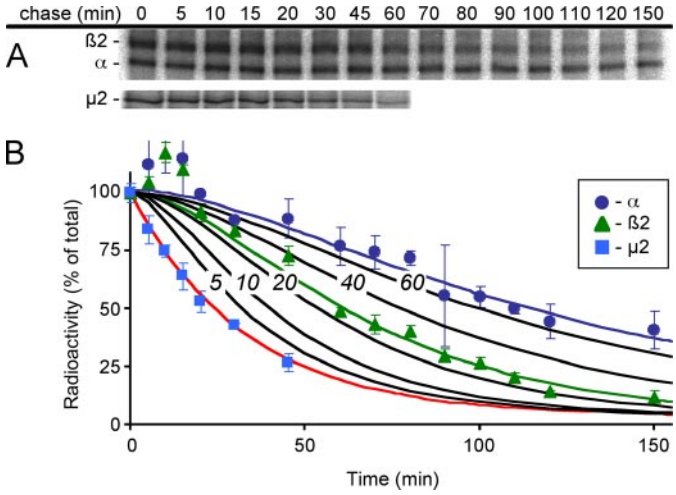

FIGURE 1. **Phosphorylation turn over of AP-2 subunits.** AP-2 was immunoprecipitated from cells that had been pulse-labeled with [^{32}P]phosphate or after pulse labeling and chase periods of the indicated duration. *A*, autoradiogram derived from SDS and urea-SDS-PAGE showing the time-dependent decay of AP-2 subunit phosphorylation. *B*, quantification of the data shown in *A*. The subunit-incorporated [^{32}P]phosphate after labeling (*0 min*) was set to 100%; all other values were related to that. The *error bars* indicate the variation between four independent experiments. The *black traces* represent model simulations of half-lives ranging from 5 to 60 min.

($t = 0$ min) or the cells were chased for different periods of time in phosphate-rich medium before AP-2 was collected. Subsequent to immunoprecipitation, AP-2 was subjected to SDS and urea-containing SDS-PAGE to resolve α-, β2-, and μ2-adaptins (Fig. 1*A*). Finally, the incorporated [^{32}P]phosphate was quantified after autoradiography, and the amount of subunit-incorporated phosphate relative to the beginning of the chase ($t = 0$ min) was plotted together with the export velocity of [^{32}P]inorganic phosphate from the cells (Fig. 1*B*, *red curve*). Interestingly, we noticed a faster phosphorylation turnover of μ2 compared with β2 and α-adaptin. To calculate realistic phosphorylation turnover rates from the raw data shown in Fig. 1*A*, the final mathematical equations had to consider the continuously decreasing probability of ^{32}P-protein rephosphorylation during the chase period (see supplemental information for a detailed description). For the turnover of μ2 phosphorylation we calculated a half-life of less than 1 min, while the two large adaptor subunits exhibited half-lives of ~25 (β2-adaptin) and ~70 min (α-adaptin). The calculated phosphorylation half-life of μ2 fits well to the turnover rate of a forming clathrin-coated vesicle (18, 19) that includes a cycle of μ2 phosphorylation and dephosphorylation in the process of high affinity binding to tyrosine-based sorting signal-containing membrane cargo proteins (11).

The phosphorylation turnover of the two AP-2 large subunits was much slower as compared with the μ2 subunit. In this context it is important to note that we did not discriminate between the potential amino acid residues involved. Using phosphoamino acid analysis, Wilde and Brodsky (20) demonstrated phosphorylation of α- and β2-adaptin only on serine residues whereas phosphorylation of tyrosine or threonine residues was not detectable. However, the pattern of phosphorylation may change upon the status of the cells analyzed. Recent data showed that stimulation of cells with epidermal growth factor resulted in phosphorylation of β2-adaptin at Tyr-6 close to the amino terminus (12). In a similar way, activation of vascular smooth muscle cells by the G-protein-coupled receptor agonist angiotensin II caused Src kinase-dependent phosphorylation of Tyr-737 located in the carboxyl-terminal appendage domain of β2-adaptin (13). The authors speculate that β2 phosphorylation in this context is required to release AP-2 from bound β-arrestin; however, the details of this regulation remain unknown. The data presented here for the phosphorylation turnover of the AP-2 subunits were obtained from unstimulated cells and resemble the experimental conditions used by Wilde and Brodsky. Although the functional role of this "basic" phosphorylation remains unclear, it may be of significance for the regulation of AP-2 binding to its many partners (1). Phosphorylation of the AP-2 large subunits in their flexible, unstructured hinge regions or their appendage domains may directly or indirectly be a prerequisite for the binding to other proteins, or to terminate such binding. Future work will need to address these possibilities on the molecular level.

Identification of a μ2-Dephosphorylating Phosphatase—The high affinity binding of μ2 to tyrosine-based sorting signals of membrane proteins requires its phosphorylation at Thr-156, mediated by the adaptor-associated kinase AAK1 and/or the cyclin G-associated kinase (10, 21, 22). In consequence, the regulatory cycle requires an antagonistic phosphatase. To characterize and finally to identify this enzyme we used immunoisolated AP-2 radiolabeled with [^{32}P]phosphate at Thr-156 as a substrate (see "Experimental Procedures" for details). Incubation of the labeled AP-2 with cytosol of different origin (*e.g.* HeLa cells or pig brain) resulted in a signal decrease, indicative of μ2 dephosphorylation (Fig. 2*A*). Small aliquots of the immunoisolated AP-2 prior and after cytosol incubation were used for the detection of α- and μ2-adaptin and revealed that equal amounts were present, clearly demonstrating that the loss of signal in the autoradiogram was the result of dephosphorylation, ruling out loss of AP-2 in the assay. When the cytosol was preincubated with sodium orthovanadate or EDTA/EGTA, dephosphorylation of μ2 was still effective, arguing against the involvement of a phosphatase dependent on divalent metal ions or a tyrosine phosphatase (not shown). In contrast, calyculin-A, microcystin, and ocadaic acid totally abolished μ2 dephosphorylation at nanomolar concentrations (not shown), indicating that a trimeric protein phosphatase like PP1 or PP2A may be a more likely candidate. Indeed, PP2A was already characterized as the enzymatic activity that mediates dephosphorylation of the μ1 subunit of the AP-1 complex (23), but no specific enzyme was identified. Because most phosphatases are predominantly cytosolic we used pig brain cytosol as a starting material for the purification of the μ2-dephosphorylating enzyme. Ammonium sulfate precipitation was first used to deplete the cytosol of a substantial number of proteins. Under these conditions, the enzyme remained in the soluble fraction as verified by dephosphorylation of AP-2 using the assay described above. The fractionated cytosol was then applied to hydrophobic interaction chromatography, followed by collection of those fractions that contained μ2-dephosphorylating enzymatic activity. The pooled fractions were further applied to strong and weak anion exchange chromatography and finally to

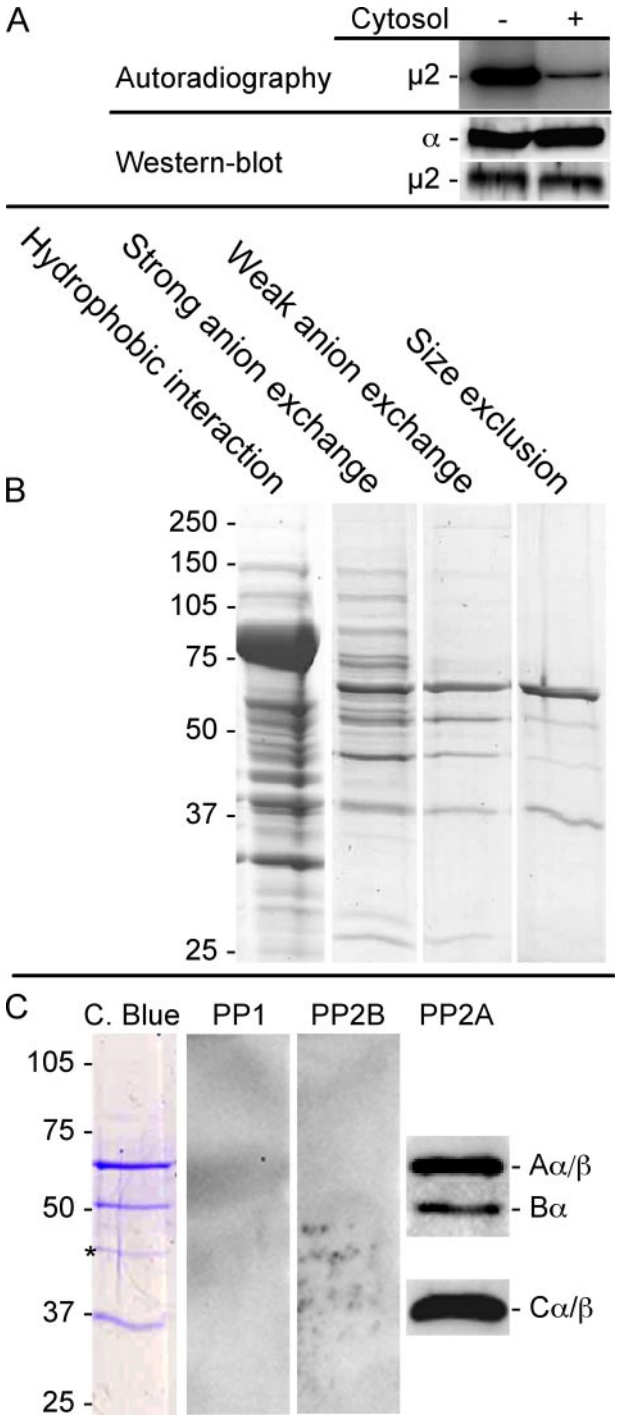

FIGURE 2. **Identification of a μ2-dephosphorylating phosphatase.** *A*, AP-2 phosphorylated on μ2 was obtained by immunoisolation from Tris-extracted CCVs that had been incubated with [γ-^{32}P]ATP. Incubation with pig brain cytosol resulted in substantial dephosphorylation of μ2. Western blot analysis for α- and μ2-adaptin revealed that no AP-2 was lost during the incubation. *B*, the μ2-dephosphorylating enzymatic activity was purified by chromatography from pig brain cytosol. All fractions of each step were tested for μ2 dephosphorylation using the assay described in *A*. Positive fractions were pooled and subjected to the next purification step. The final size exclusion chromatography yielded a pool of activity, which was recovered from two fractions eluting with a molecular mass of ~200 kDa. *C*, the Coomassie stain of the purified phosphatase activity is shown in the *first lane*. Three of the purified proteins were identified by peptide mass fingerprinting as the Aβ, Bα, and Cβ subunits of a PP2A holoenzyme; protein 4 (*asterisk*) was identified as actin. Western blot analysis of the purified enzyme revealed the absence of PP1 (*lane 2*) and PP2B/calcineurin (*lane 3*), whereas the three subunits of PP2A were positively identified (*lane 4*; the specificity of the antibodies is indicated on the *right*).

size exclusion chromatography. At this step the μ2-dephosphorylating activity eluted in a single small peak that contained four proteins (Fig. 2*B*), which were subjected to peptide mass fingerprinting. With Mowse scores ≥200, one of the proteins was identified as actin (Fig. 2*C*, *asterisk*); the other three proteins were identified as the Aβ, Bα, and Cβ subunits of PP2A. In conclusion, we succeeded in the first purification of a PP2A holoenzyme that mediates dephosphorylation of the μ2 subunit of AP-2.

The purified enzyme preparation was free of any contamination by PP1 or PP2B as verified by Western blotting, whereas each PP2A subunit was unequivocally detected by antibodies of the respective specificity (Fig. 2*C*). Based on the protein-specific activity toward μ2, our purification resulted in a >5,000-fold enrichment of the PP2A holoenzyme. Between different preparations we noticed that the PP2A A and C subunits were mostly present in stoichiometric amounts, while the amount of the B subunit was not equivalent when analyzed by Coomassie staining of the proteins.

The comparison of the purified enzyme with commercially available dimeric and trimeric PP2A showed that only the latter was able to dephosphorylate μ2, suggesting that presence of the B subunit in the holoenzyme is important (Fig. 3*A*). As expected for a classical PP2A, the enzyme preparation was sensitive to the known inhibitors calyculin-A and ocadaic acid, with K_i values for the dephosphorylation of μ2 of 8 and 30 nM, respectively (Fig. 3*C*). In addition, the dephosphorylation of μ2 could be effectively inhibited by a synthetic 16-mer peptide derived from μ2 and including phosphorylated Thr-156, whereas addition of a non-related peptide had no significant effect (Fig. 3*D*). To rule out that any other contaminating phosphatase activity was dephosphorylating the AP-2 μ2 subunit, we applied aliquots of the PP2A purification to the depletion with either nonspecific mouse IgG or monoclonal anti-PP2A C subunit IgG coupled to protein-A-agarose. As shown in Fig. 3*B*, no PP2A was captured with control IgG, whereas the anti-C subunit beads were able to deplete PP2A from the input almost quantitatively. The supernatants of both depletions as well as a non-treated control were then used in the μ2-dephosphorylation assay. The supernatant of the IgG beads as well as the non-treated PP2A preparation exhibited equally high dephosphorylation activities (30 and 20% remaining phospho-μ2, respectively), whereas the anti-PP2A supernatant lost its enzymatic activity (95% phospho-μ2). We therefore conclude that indeed the PP2A holoenzyme we identified dephosphorylates μ2 and not any other enzymatic impurity.

Knock Down of PP2A Bα Affects the Phosphorylation Status of μ2—The results described above show that the purified PP2A holoenzyme mediates μ2 dephosphorylation *in vitro*. To analyze the significance of our findings for living cells, we suppressed the expression of the PP2A Bα subunit in HeLa cells by vector-based RNAi. In this context one should note that the highly conserved PP2A A subunit associates with the C subunit in a dimeric core enzyme that is thought to lack specificity for substrate and intracellular localization (24, 25). Both functions are mediated by the B subunit family of proteins. Four such families have been characterized, each comprising four or more members. Because some of the B-proteins can be expressed as

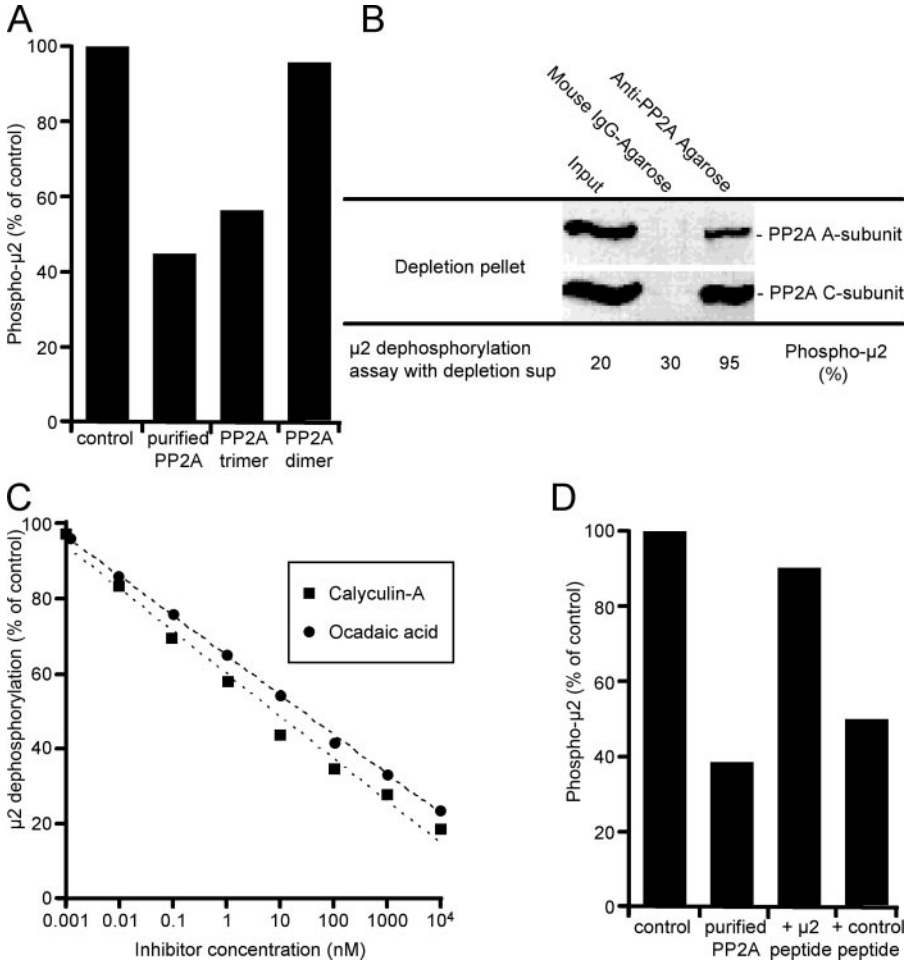

FIGURE 3. **Characterization of the μ2-dephosphorylating PP2A.** The purified PP2A holoenzyme was compared with commercially available dimeric and trimeric forms of PP2A in the μ2 dephosphorylation assay. Note that only the trimeric holoenzyme was active (*A*). To further prove that dephosphorylation of μ2 was mediated by the purified PP2A and not by a contaminating enzyme, a 1-μg sample of the PP2A preparation (*Input*) was subjected to depletion with either control IgG beads or beads coated with a monoclonal antibody specific for the PP2A catalytic subunit (*B*). After depletion, the beads were collected and tested for PP2A by Western blotting using two different antibodies. No PP2A was captured by control beads, but only by anti-PP2A beads. The supernatants of the depletion and a non-treated control were used for μ2 dephosphorylation. Only the supernatants of the control and the IgG beads were active, whereas that of the anti-PP2A beads lost all μ2-phosphorylating activity. As shown in *C* and *D*, the activity of the purified enzyme was inhibited by increasing concentrations of two known PP2A inhibitors (*C*) and by addition of a synthetic Thr-156-phosphorylated μ2 peptide, but not by a non-related peptide (*D*), demonstrating that the AP-2 μ2 subunit is a substrate of the purified PP2A holoenzyme.

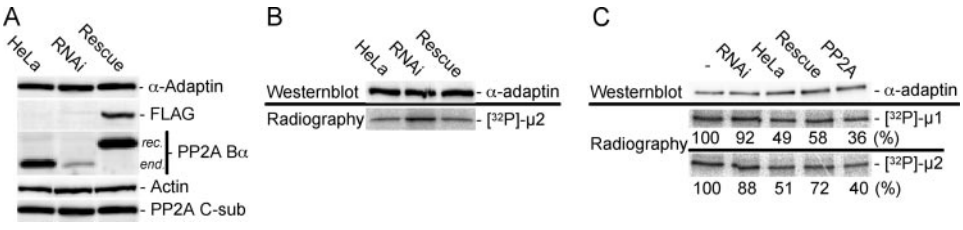

FIGURE 4. **Knock down of PP2A Bα impairs μ subunit dephosphorylation.** As shown in *A*, expression of the endogenous Bα subunit of PP2A was efficiently knocked down in HeLa cells by RNAi (see "Experimental Procedures" for details), while three other marker proteins were not affected. Rescue cells express a recombinant, RNAi-insensitive 3× FLAG-tagged Bα subunit as indicated by the slight shift in mobility and its detection by anti-FLAG antibodies (compare *lanes 2* and *3*). When equal amounts of AP-2 (Western blot in *B*) were precipitated from ^{32}P-labeled cells, we noticed a 2-fold increase of phospho-μ2 in RNAi cells (radiography in *B*), suggesting an inhibition of the involved PP2A. Expression of the RNAi-insensitive 3× FLAG-tagged Bα was sufficient to restore the original phosphorylation pattern of μ2. In support of these results, cytosol prepared from Bα RNAi cells was impaired in μ2 dephosphorylation compared with cytosol from rescue cells and HeLa cells or to incubation with the purified PP2A (*C*). Note that PP2A dephosphorylates not only μ2 but also the AP-1 μ1 subunit. The numbers represent the remaining amount of phospho-μ substrate after cytosol incubation as % of the untreated control in *lane 1*.

splice variants, the theoretical number of PP2A holoenzymes exceeds 70, each consisting of one of the two A subunits (α or β), one of the two catalytic C subunits (α or β), and one of the many B subunits (26–28). Because the holoenzyme purified by us contained the Bα subunit of the B55 family (29), it was the obvious knockdown target in HeLa cells. As shown in Fig. 4*A*, we could efficiently and specifically suppress Bα expression (~5% residual protein), while neither the PP2A catalytic subunit nor other control proteins were affected. As a control for the specificity of suppression of the Bα subunit, we generated a recombinant subunit that was insensitive to RNAi, because the cDNA was lacking the RNAi target sequences located in the 3′-untranslated region. The recombinant tagged Bα subunit had a 50-amino acid amino terminal extension including a 3× FLAG tag and was expressed in Bα RNAi cells (*Rescue*) as confirmed by detection with FLAG tag-specific antibodies (Fig. 4*A*, *lane 3*). As shown with antibodies against endogenous Bα, the recombinant subunit has a slightly higher molecular mass, was exclusively detectable in the rescue cells, and was slightly overexpressed (Fig. 4*A*, compare *lanes 1–3*). We next labeled cells with [^{32}P]phosphate and used equal amounts of protein for precipitation of AP-2. As indicated in Fig. 4*B*, the phospho-μ2 signal was increased by 2-fold in AP-2 derived from the RNAi cells, even though the same amounts of AP-2 were gained from all cell types. Note that the original degree of μ2 phosphorylation was restored in RNAi cells expressing the recombinant 3× FLAG Bα subunit, indicative of its integration into functional PP2A holoenzymes that dephosphorylate AP-2. This notion was further corroborated by co-immunoprecipitation of the PP2A A and C subunits with FLAG tag-specific antibodies and by detection of the recombinant Bα subunit in a pull-down with agarose-immobilized microcystin, which was used as an

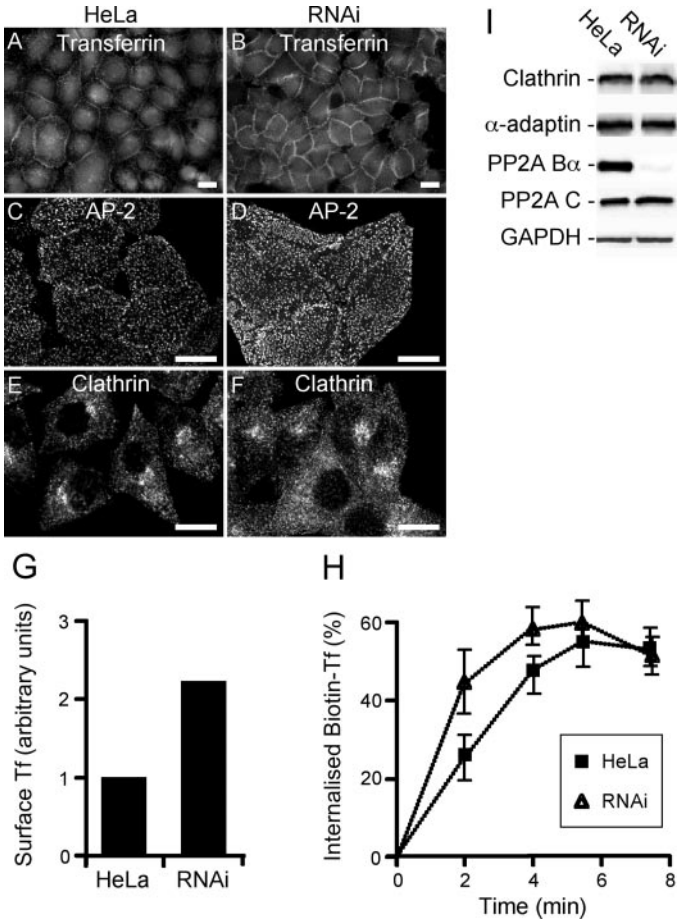

FIGURE 5. **Knock down of PP2A Bα perturbs transferrin endocytosis.** HeLa cells (*A*, *C*, *E*) and PP2A Bα RNAi cells (*B*, *D*, *F*) were incubated on ice with Alexa 546-conjugated human transferrin (*A* and *B*) to label the transferrin receptor population present at the plasma membrane. Note that the cell surface-staining intensity was stronger in the RNAi cells. Additionally, the punctate pattern of the two main CCV proteins AP-2 (*C* and *D*) and clathrin (*E* and *F*) was more pronounced, indicative of a higher number of coated structures. Quantification of the transferrin signal intensities along plasma membrane profiles revealed a >2-fold increase in the amount at the plasma membrane (*G*). Consistent with this finding, the uptake of biotinylated transferrin in RNAi cells was faster in the initial phase of endocytosis (*H*). *Error bars* represent the variation between four independent experiments. A fraction of the cells was analyzed by Western blotting to verify the effectiveness of RNAi (*I*).

affinity matrix for the capture of PP2A (see supplemental Fig. S1). We therefore conclude that the pool of AP-2 phosphorylated at μ2 is enlarged in Bα RNAi cells. Consistent with this result, the cytosol from RNAi cells lost its μ2-dephosphorylating activity (Fig. 4*C*) as compared with cytosol from HeLa cells and rescue cells expressing recombinant Bα, or after incubation with the purified PP2A. In the same set of experiments we used ^{32}P-labeled AP-1 as a substrate, which was also dephosphorylated by the purified PP2A, but not by the RNAi cell-derived cytosol. This observation is consistent with the results of the Kornfeld group, who previously showed that dephosphorylation of the AP-1 μ1 subunit is PP2A-mediated (23), and suggests that PP2A is an important regulatory enzyme of clathrin adaptors.

Membrane protein binding in the process of clathrin-coated vesicle formation at the plasma membrane is one of the important functions of AP-2. We therefore analyzed the localization of clathrin and AP-2 in HeLa and PP2A Bα RNAi cells and monitored whether RNAi had any impact on endocytic processes. As shown in Fig. 5, we noticed that the typical punctate pattern of AP-2 and clathrin was more pronounced in the RNAi cells (compare *panel C* to *F*). Interestingly, the surface expression of the Tf receptor, which is widely used as a readout for functional analyses of endocytic proteins (30–32), was also increased by 2-fold in the RNAi cells as indicated after incubation with fluorescent transferrin on ice (compare Fig. 5, *A* and *B*, quantification in *G*). The endocytosis of transferrin reached similar levels (60% within 6 min) in HeLa and RNAi cells, but the latter exhibited a significant higher rate of uptake (Fig. 5*D*). The amount of intracellular-detectable transferrin slightly decreased between 6 and 8 min, most likely because some transferrin already recycled back to the cell surface within this period. In contrast to our findings on the internalization of transferrin, the receptor-mediated uptake of fluorescent low density lipoprotein and the fluid phase endocytosis of rhodamine-labeled dextran were not significantly affected when analyzed by immunofluorescence (not shown). In conclusion, our results show that knock down of the PP2A Bα subunit affects the amount of AP-2 and clathrin that was localized to coated structures; however, endocytic processes were only marginally affected. One explanation might be that imbalances in the regulatory cycle of AP-2 phosphorylation and dephosphorylation may only have a small impact on the endocytic machinery in general. Still, we are just beginning to explore the mechanisms by which kinases and phosphatases regulate the functions of endocytic proteins. Several kinases as well as PP1, PP2A, and other phosphatases are present in coated vesicle preparations (33–36), suggesting that the activities of these counteracting enzymes have to be tightly controlled within the short period of coated vesicle formation. Interestingly, the adaptor-associated kinase AAK1 is active in a protein preparation liberated from clathrin-coated vesicles by Tris extraction and easily phosphorylates AP-2 when ATP is added. In contrast, the PP2A in the same preparation is inactive and unable to dephosphorylate AP-2.[5] Whether the PP2A activity is regulated by post-translational modification(s), how the enzyme is recruited to forming clathrin-coated vesicles, and whether it has other substrates apart from AP-2 are some of the questions that we need to address to get a deeper insight into the functional regulation of endocytosis.

Acknowledgments—We thank Christina Kiecke and Andrea Rüger for expert technical assistance, Nicole Eiselt for expertise in mass spectrometry-based protein identification, and Frank Konietschke (Institute for Medical Statistics, Göttingen) for verification of the mathematics of our model.

REFERENCES

1. Ungewickell, E. J., and Hinrichsen, L. (2007) *Curr. Opin. Cell Biol.* **9,** 417–425
2. Cousin, M. A., and Robinson, P. J. (2001) *Trends Neurosci.* **24,** 659–665
3. Flett, A., Semerdjieva, S., Jackson, A. P., and Smythe, E. (2005) *Biochem. Soc. Symp.* **72,** 65–70
4. Olusanya, O., Andrews, P. D., Swedlow, J. R., and Smythe, E. (2001) *Curr.*

[5] D. Ricotta and S. Höning, unpublished observation.

Biol. **11,** 896–900
5. Ricotta, D., Conner, S. D., Schmid, S. L., von Figura, K., and Höning, S. (2002) *J. Cell Biol.* **156,** 791–795
6. Conner, S. D., and Schmid, S. L. (2002) *J. Cell Biol.* **156,** 921–929
7. Greener, T., Zhao, X., Nojima, H., Eisenberg, E., and Greene, L. E. (2000) *J. Biol. Chem.* **275,** 1365–1370
8. Umeda, A., Meyerholz, A., and Ungewickell, E. (2000) *Eur. J. Cell Biol.* **79,** 336–342
9. Lee, D. W., Zhao, X., Zhang, F., Eisenberg, E., and Greene, L. E. (2005) *J. Cell Sci.* **118,** Pt. 18, 4311–4321
10. Henderson, D. M., and Conner, S. D. (2007) *Mol. Biol. Cell* **18,** 2698–2706
11. Höning, S., Ricotta, D., Krauss, M., Spate, K., Spolaore, B., Motley, A., Robinson, M., Robinson, C., Haucke, V., and Owen, D. J. (2005) *Mol. Cell* **18,** 519–531
12. Huang, F., Jiang, X., and Sorkin, A. (2003) *J. Biol. Chem.* **278,** 43411–43417
13. Fessart, D., Simaan, M., Zimmerman, B., Comeau, J., Hamdan, F. F., Wiseman, P. W., Bouvier, M., and Laporte, S. A. (2007) *J. Cell Sci.* **120,** Pt. 10, 1723–1732
14. Conner, S. D., and Schmid, S. L. (2005) *J. Biol. Chem.* **280,** 21539–21544
15. Fingerhut, A., von Figura, K., and Höning, S. (2001) *J. Biol. Chem.* **276,** 5476–5482
16. Ahle, S., and Ungewickell, E. (1986) *EMBO J.* **5,** 3143–3149
17. Shevchenko, A., Wilm, M., Vorm, O., Jensen, O. N., Podtelejnikov, A. V., Neubauer, G., Shevchenko, A., Mortensen, P., and Mann, M. (1996) *Biochem. Soc. Trans.* **24,** 893–896
18. Ehrlich, M., Boll, W., Van Oijen, A., Hariharan, R., Chandran, K., Nibert, M. L., and Kirchhausen, T. (2004) *Cell* **118,** 591–605
19. Zoncu, R., Perera, R. M., Sebastian, R., Nakatsu, F., Chen, H., Balla, T., Ayala, G., Toomre, D., and De Camilli, P. V. (2007) *Proc. Natl. Acad. Sci. U. S. A.* **104,** 3793–3798
20. Wilde, A., and Brodsky, F. M. (1996) *J. Cell Biol.* **135,** 635–645
21. Zhang, C. X., Engqvist-Goldstein, A. E., Carreno, S., Owen, D. J., Smythe, E., and Drubin, D. G. (2005) *Traffic* **6,** 1103–1113
22. Lee, D. W., Wu, X., Eisenberg, E., and Greene, L. E. (2006) *J. Cell Sci.* **119,** Pt. 17, 3502–3512
23. Ghosh, P., and Kornfeld, S. (2003) *J. Cell Biol.* **160,** 699–708
24. Janssens, V., and Goris, J. (2001) *Biochem. J.* **353,** Pt. 3, 417–439
25. Virshup, D. M. (2000) *Curr. Opin. Cell Biol.* **12,** 180–185
26. Goldberg, Y. (1999) *Biochem. Pharmacol.* **57,** 321–328
27. Cho, U. S., and Xu, W. (2007) *Nature* **445,** 53–57
28. Xu, Y., Xing, Y., Chen, Y., Chao, Y., Lin, Z., Fan, E., Yu, J. W., Strack, S., Jeffrey, P. D., and Shi, Y. (2006) *Cell* **127,** 1239–1251
29. Longin, S., Zwaenepoel, K., Louis, J. V., Dilworth, S., Goris, J., and Janssens, V. (2007) *J. Biol. Chem.* **282,** 26971–26980
30. Motley, A. M., Berg, N., Taylor, M. J., Sahlender, D. A., Hirst, J., Owen, D. J., and Robinson, M. S. (2006) *Mol. Biol. Cell* **17,** 5298–5308
31. Buss, F., Arden, S. D., Lindsay, M., Luzio, J. P., and Kendrick-Jones, J. (2001) *EMBO J.* **20,** 3676–3684
32. Keyel, P. A., Mishra, S. K., Roth, R., Heuser, J. E., Watkins, S. C., and Traub, L. M. (2006) *Mol. Biol. Cell* **17,** 4300–4317
33. Pauloin, A., Loeb, J., and Jolles, P. (1984) *Biochim. Biophys. Acta* **799,** 238–245
34. Korolchuk, V., and Banting, G. (2003) *Biochem. Soc. Trans.* **31,** Pt. 4, 857–860
35. Borner, G. H., Harbour, M., Hester, S., Lilley, K. S., and Robinson, M. S. (2006) *J. Cell Biol.* **175,** 571–578
36. Blondeau, F., Ritter, B., Allaire, P. D., Wasiak, S., Girard, M., Hussain, N. K., Angers, A., Legendre-Guillemin, V., Roy, L., Boismenu, D., Kearney, R. E., Bell, A. W., Bergeron, J. J., and McPherson, P. S. (2004) *Proc. Natl. Acad. Sci. U. S. A.* **101,** 3833–3838